Energetics and scattering at fourth post-Minkowskian order

Mohammed Khalil

Max Planck Institute for Gravitational Physics (Albert Einstein Institute)
University of Maryland, College Park

in collaboration with
Alessandra Buonanno, Jan Steinhoff, Justin Vines
[arXiv:2204.05047]

DESY, Zeuthen
May 12, 2022

The need for accurate waveforms

- Accurate waveform models are crucial in searching for gravitational-wave signals and inferring their parameters.
- Numerical relativity (NR) waveforms are computationally expensive, making analytical approximations important.

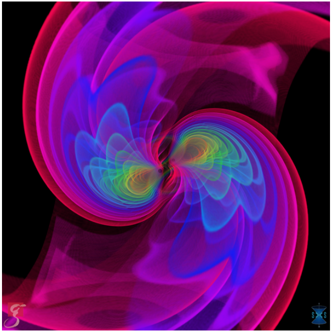

[Ossokine, Buonanno, SXS]

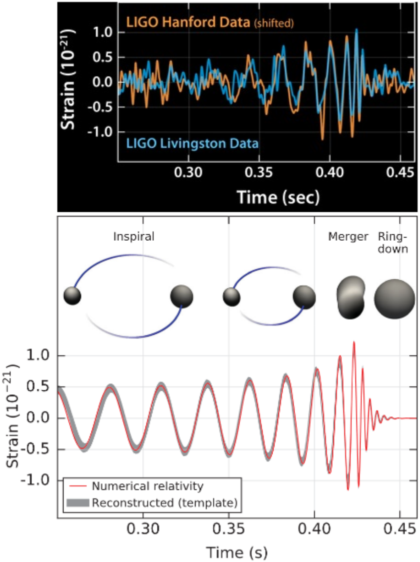

[LIGO Scientific Collaboration 2016]

Analytical approximations for the inspiral

Post-Newtonian (PN)	Post-Minkowskian (PM)	Gravitational Self-Force (GSF)
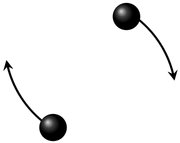	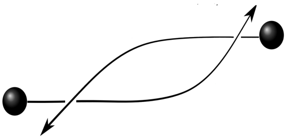	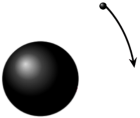
$\frac{v^2}{c^2} \sim \frac{GM}{rc^2} \ll 1$	$\frac{GM}{rc^2} \ll 1$	$\frac{m_1}{m_2} \ll 1$

		0PN	1PN	2PN	3PN	4PN	5PN	$\cdots$
0PM	1	v^2	v^4	v^6	v^8	v^{10}	v^{12}	$\cdots$
1PM (G^1)		$1/r$	v^2/r	v^4/r	v^6/r	v^8/r	v^{10}/r	$\cdots$
2PM (G^2)			$1/r^2$	v^2/r^2	v^4/r^2	v^6/r^2	v^8/r^2	$\cdots$
3PM (G^3)				$1/r^3$	v^2/r^3	v^4/r^3	v^6/r^3	$\cdots$
4PM (G^4)					$1/r^4$	v^2/r^4	v^4/r^4	$\cdots$
5PM (G^5)						$1/r^5$	v^2/r^5	$\cdots$
6PM (G^6)							$1/r^6$	$\cdots$

Regions of applicability of NR and the approximation methods

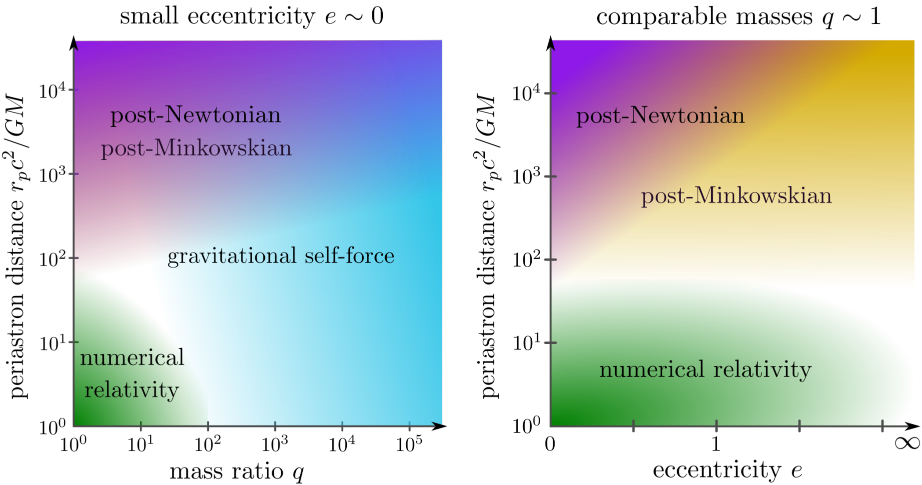

- All GW detections so far are consistent with bound-orbit inspirals, with expected event rates for hyperbolic encounters from 0.001 to 0.39 per year for upcoming LIGO-Virgo-KAGRA runs. [Mukherjee, Mitra, Chatterjee 2010.00916]

Outline

- Overview of PM results for the conservative dynamics
- Compare PM binding energy and scattering angle with NR
- Incorporate PM results in effective-one-body (EOB) Hamiltonians

3PM conservative dynamics

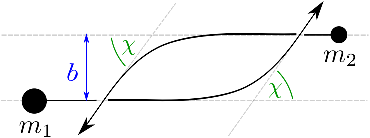

- 1PM results were obtained by [Bertotti '56], with the 2PM scattering angle first computed by [Westpfahl '85].
- The scattering angle contains the full gauge-invariant information for the conservative binary dynamics. [Damour 1609.00354, 1710.10599]
- 3PM conservative dynamics
  - derived using scattering amplitudes [Bern, Cheung, Roiban, Shen, Solon, Zeng 1901.04424]
  - reproduced using Feynman diagrams and effective field theory approach [Cheung, Solon 2003.08351], [Kälin, Liu, Porto 2007.04977]
  - agrees with 6PN results [Blümlein, Maier, Marquard, Schäfer 2003.07145], [Bini, Damour, Geralico 2004.05407]
  - has a mass singularity in the high-energy limit, cancels with radiative contribution [Di Vecchia, Heissenberg, Russo, Veneziano 2008.12743], [Damour 2010.01641]

4PM conservative dynamics for hyperbolic orbits

- Nonlocal-in-time (tail) effects contribute to the conservative dynamics at 4PM/4PN, due to GWs emitted at earlier times and backscattered off the spacetime curvature.

- 4PM conservative dynamics derived for hyperbolic orbits using scattering amplitudes, and exhibits a simple mass dependence for the scattering angle.
  [Bern, Parra-Martinez, Roiban, Ruf, Shen, Solon, Zeng 2101.07254, 2112.10750]

- Derived independently using EFT methods, but has been argued to be missing additional contributions of $\mathcal{O}(\nu^2)$. [Dlapa, Kälin, Liu, Porto 2106.08276, 2112.11296]

4PM conservative dynamics for hyperbolic orbits

- Nonlocal-in-time (tail) effects contribute to the conservative dynamics at 4PM/4PN, due to GWs emitted at earlier times and backscattered off the spacetime curvature.
- 4PM conservative dynamics derived for hyperbolic orbits using scattering amplitudes, and exhibits a simple mass dependence for the scattering angle.
[Bern, Parra-Martinez, Roiban, Ruf, Shen, Solon, Zeng 2101.07254, 2112.10750]
- Derived independently using EFT methods, but has been argued to be missing additional contributions of $\mathcal{O}(\nu^2)$. [Dlapa, Kälin, Liu, Porto 2106.08276, 2112.11296]
- Agrees with 6PN results of [Bini, Damour, Geralico 2003.11891, 2007.11239], but disagrees in one term with 5PN results of [Blümlein, Maier, Marquard, Schäfer 2110.13822]
- Disagreement might be due to the definition of conservative versus radiative contributions; terms quadratic in radiation reaction start at 5PN/4PM.
- At 5PN, the difference is $\sim \nu^2 v^6 / J^4$, which has a negligible effect on our study, since all binary configurations considered have velocities $\lesssim 0.5$.

Mass dependence of the scattering angle

- Based on the structure of the PM expansion, symmetries and dimensional analysis, the scattering angle has the mass dependence [Damour 1912.02139]

$$
\begin{aligned}
\frac{M}{E}\chi = {} & \frac{GM}{b}\mathsf{X}_1 + \left(\frac{GM}{b}\right)^2 \mathsf{X}_2 \\
& + \left(\frac{GM}{b}\right)^3 \left[\mathsf{X}_3 + \nu \mathsf{X}_3^\nu\right] + \left(\frac{GM}{b}\right)^4 \left[\mathsf{X}_4 + \nu \mathsf{X}_4^\nu\right] \\
& + \left(\frac{GM}{b}\right)^5 \left[\mathsf{X}_5 + \nu \mathsf{X}_5^\nu + \nu^2 \mathsf{X}_5^{\nu^2}\right] + \dots
\end{aligned}
$$

$$
M \equiv m_1 + m_2, \qquad 0 \leq \left(\nu \equiv \frac{m_1 m_2}{M^2}\right) \leq \frac{1}{4}
$$

- This structure made it possible to derive new PN results from GSF
  - partial 5PN and 6PN [Bini, Damour, Geralico 2003.11891, 2004.05407]
  - complete 4.5PN spin-orbit and 5PN aligned spin$_1$-spin$_2$ [Antonelli, Kavanagh, **MK**, Steinhoff, Vines 2003.11391, 2010.02018]
  - partial 5.5PN spin-orbit [**MK** 2110.12813]

From scattering to bound orbits for local-in-time dynamics

- Scattering informs bound orbits; scattering angle related to periastron advance

[Kälin, Porto 1910.03008, 1911.09130]

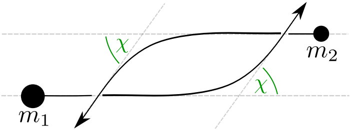

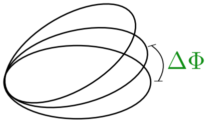

$$\Delta\Phi(E,J) = \chi(E,J) + \chi(E,-J)$$

- General map between bound and unbound observables

[Saketh, Vines, Steinhoff, Buonanno 2109.05994], [Cho, Kälin, Porto 2112.03976]

$$\mathrm{O}_{\text{bound}}(E,J) = 2\int_{r_{\text{min}}}^{r_{\text{max}}} f(r,E,J)\mathrm{d}r, \qquad \mathrm{O}_{\text{unbound}}(E,J) = 2\int_{r_{\text{min}}}^{\infty} f(r,E,J)\mathrm{d}r$$

$$\mathrm{O}_{\text{bound}}(E,J) = \mathrm{O}_{\text{unbound}}(E,J) + \theta(f)\mathrm{O}_{\text{unbound}}(E,-J)$$

$\theta(f) = \pm 1$ if f is odd/even in J.

For $\Delta\Phi$ and χ, $f = \partial p_r/\partial J$

Nonlocal contribution at 4PN

- Total action is split into local and nonlocal-in-time pieces $S_{\text{tot}}^{\text{nPN}} = S_{\text{loc}}^{\text{nPN}} + S_{\text{nonloc}}^{\text{nPN}}$

[Damour, Jaranowski, Schäfer 1401.4548, 1502.07245]

$$S_{\text{nonloc}}^{\text{4PN}} = \frac{GM}{c^3} \int \mathrm{d}t \, \mathsf{Pf}_{2s/c} \int \frac{\mathrm{d}t'}{|t-t'|} \mathcal{F}^{\text{2.5PN}}(t,t') \equiv - \int \mathrm{d}t \, \delta H_{\text{nonloc}}^{\text{4PN}}(t)$$

The time-symmetric GW energy flux $\mathcal{F}^{\text{2.5PN}}(t,t') = \frac{G}{c^5} \left[\frac{1}{5} I_{ij}^{(3)}(t) I_{ij}^{(3)}(t') + \dots \right]$

- Nonlocal 4PN Hamiltonian (define $\tau \equiv t' - t$)

$$\delta H_{\text{nonloc}}^{\text{4PN}}(t) = -\frac{GM}{c^3} \mathsf{Pf}_{2s/c} \int \frac{\mathrm{d}\tau}{|\tau|} \mathcal{F}^{\text{2.5PN}}(t, t+\tau) + 2 \frac{GM}{c^3} \mathcal{F}^{\text{2.5PN}}(t,t) \ln\left(\frac{r}{s}\right)$$

Nonlocal contribution at 4PN

- Total action is split into local and nonlocal-in-time pieces $S^{\text{nPN}}_{\text{tot}} = S^{\text{nPN}}_{\text{loc}} + S^{\text{nPN}}_{\text{nonloc}}$

[Damour, Jaranowski, Schäfer 1401.4548, 1502.07245]

$$S^{\text{4PN}}_{\text{nonloc}} = \frac{GM}{c^3} \int \mathrm{d}t \, \mathrm{Pf}_{2s/c} \int \frac{\mathrm{d}t'}{|t-t'|} \mathcal{F}^{\text{2.5PN}}(t,t') \equiv - \int \mathrm{d}t \, \delta H^{\text{4PN}}_{\text{nonloc}}(t)$$

The time-symmetric GW energy flux $\mathcal{F}^{\text{2.5PN}}(t,t') = \frac{G}{c^5} \left[\frac{1}{5} I^{(3)}_{ij}(t) I^{(3)}_{ij}(t') + \dots \right]$

- Nonlocal 4PN Hamiltonian (define $\tau \equiv t' - t$)

$$\delta H^{\text{4PN}}_{\text{nonloc}}(t) = -\frac{GM}{c^3} \mathrm{Pf}_{2s/c} \int \frac{\mathrm{d}\tau}{|\tau|} \mathcal{F}^{\text{2.5PN}}(t,t+\tau) + 2\frac{GM}{c^3} \mathcal{F}^{\text{2.5PN}}(t,t) \ln\left(\frac{r}{s}\right)$$

- Nonlocal contribution to the scattering angle [Bini, Damour 1706.06877]

$$\chi_{\text{nonloc}} = \frac{1}{\nu} \frac{\partial}{\partial J} W_{\text{nonloc}}(E,J), \qquad W_{\text{nonloc}} = \int dt \, \delta H_{\text{nonloc}},$$

- Integral is computed in small/large eccentricity expansion for bound/unbound orbits.

$$\delta H^{\text{4PN}}_{\text{nonloc}} \sim \frac{G^5}{r^5} + \frac{G^4 p_r^2}{r^4} + \frac{G^3 p_r^4}{r^3} + \dots \sim e^0 + e^2 + \dots$$

$$\chi_{\text{nonloc}} \sim \frac{G^4}{J^4} + \frac{G^5}{J^5} + \frac{G^6}{J^6} + \dots \qquad \sim \frac{1}{e^4} + \frac{1}{e^5} + \dots$$

- No clear relation between bound and unbound orbits for nonlocal contributions

[Cho, Kälin, Porto 2112.03976]

4PM radial action and Hamiltonian

- Radial action

$$I_{r,\text{4PM}}^{\text{hyp}} = I_{r,\text{3PM}} - \frac{\pi G^4 M^7 \nu^2 p^2}{8 E J^3} \left[\mathcal{M}_4^{\text{p}} + \nu \left(4 \mathcal{M}_4^{\text{t}} \ln \frac{\sqrt{\sigma^2 - 1}}{2} + \mathcal{M}_4^{\pi^2} + \mathcal{M}_4^{\text{rem}} \right) \right]$$

terms $\mathcal{M}_4^{\cdot\cdot}$ are directly related to parts of the scattering amplitude [Bern+ '21]

$$\mathcal{M}_4^{\mathrm{p}} = -\frac{35\left(1 - 18\sigma^2 + 33\sigma^4\right)}{8\left(\sigma^2 - 1\right)},$$

$$\sigma \equiv \frac{p_1 \cdot p_2}{m_1 m_2}$$

$$\mathcal{M}_4^{\mathrm{t}} = r_1 + r_2 \log\left(\tfrac{\sigma+1}{2}\right) + r_3 \frac{\operatorname{arccosh}(\sigma)}{\sqrt{\sigma^2 - 1}},$$

$$\mathcal{M}_4^{\pi^2} = r_4 \pi^2 + r_5\, \mathrm{K}\left(\tfrac{\sigma-1}{\sigma+1}\right) \mathrm{E}\left(\tfrac{\sigma-1}{\sigma+1}\right) + r_6\, \mathrm{K}^2\left(\tfrac{\sigma-1}{\sigma+1}\right) + r_7\, \mathrm{E}^2\left(\tfrac{\sigma-1}{\sigma+1}\right),$$

$$\begin{aligned}\mathcal{M}_4^{\mathrm{rem}} = {} & r_8 + r_9 \log\left(\tfrac{\sigma+1}{2}\right) + r_{10} \tfrac{\operatorname{arccosh}(\sigma)}{\sqrt{\sigma^2-1}} + r_{11} \log(\sigma) + r_{12} \log^2\left(\tfrac{\sigma+1}{2}\right) + r_{13} \tfrac{\operatorname{arccosh}(\sigma)}{\sqrt{\sigma^2-1}} \log\left(\tfrac{\sigma+1}{2}\right) + r_{14} \tfrac{\operatorname{arccosh}^2(\sigma)}{\sigma^2-1} \\ & + r_{15} \operatorname{Li}_2\left(\tfrac{1-\sigma}{2}\right) + r_{16} \operatorname{Li}_2\left(\tfrac{1-\sigma}{1+\sigma}\right) + r_{17} \tfrac{1}{\sqrt{\sigma^2-1}} \left[\operatorname{Li}_2\left(-\sqrt{\tfrac{\sigma-1}{\sigma+1}}\right) - \operatorname{Li}_2\left(\sqrt{\tfrac{\sigma-1}{\sigma+1}}\right)\right].\end{aligned}$$

- Scattering angle

$$\chi = -\frac{\partial I_r^{\text{hyp}}}{\partial J}$$

- Hamiltonian in isotropic gauge (no explicit dependence on p_r or J)

$$H_{\text{4PM}}^{\text{hyp}} = \sqrt{m_1^2 + p^2} + \sqrt{m_2^2 + p^2} + \sum_{n=1}^{4} \frac{G^n}{r^n} c_n,$$

Binding energy from PM-expanded Hamiltonian

- Binding energy $\bar{E} \equiv H - M$, calculated assuming exact circular orbits.
- Set $p_r = 0$ in H, and solve $\dot{p}_r = \partial H / \partial r = 0$ for J at each point in r.
- Plot $H(J, r) - M$ versus orbital frequency $\Omega(J, r) = \partial H / \partial J$.
- NR energy $\bar{E}_{\text{NR}} \equiv E_{\text{ADM}} - E_{\text{rad}} - M$
- 4PM contains full 3PN, which gives a significant improvement over 2PN.

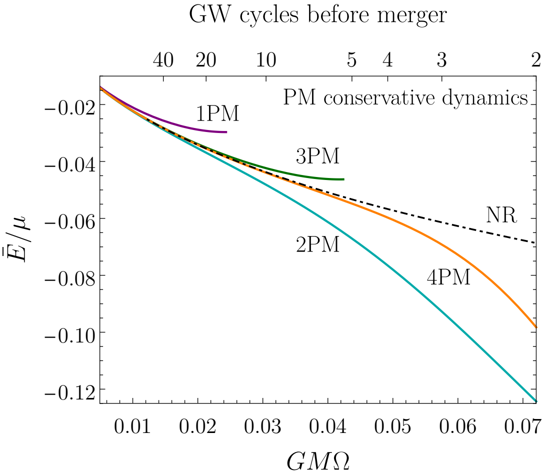

NR data for binding energy from [Ossokine, Dietrich, Foley, Katebi, Lovelace 1712.06533]

PN-expanded binding energy for elliptic vs. hyperbolic orbits

- Calculated 6PN(4PM) binding energy for hyperbolic orbits from $H^{\text{hyp}}_{\text{4PM}}$.
- Calculated 6PN(4PM) binding energy for bound orbits, by transforming 6PN EOB Hamiltonian [Bini,Damour,Geralico 2004.05407] to isotropic gauge and truncating at 4PM.
- Difference at 4PN, $\bar{E}^{\text{iso,hyp}}_{\text{4PN(4PM)}} - \bar{E}^{\text{iso,ell}}_{\text{4PN(4PM)}} \simeq 15\nu x^5$
  That coefficient is -113 in $\bar{E}^{\text{iso,ell}}_{\text{4PN(4PM)}}$ and -98 in $\bar{E}^{\text{iso,hyp}}_{\text{4PN(4PM)}}$.

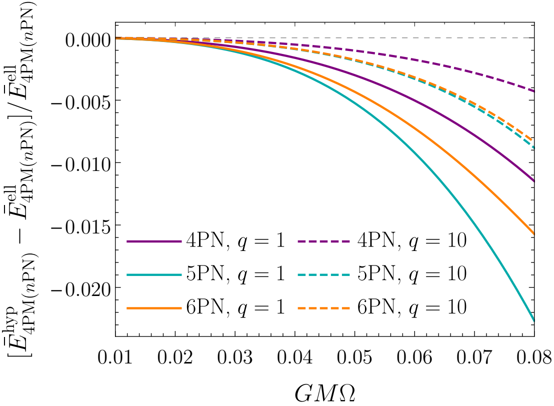

4PM complemented with bound-orbit PN information

- Complemented the 4PM Hamiltonian with bound-orbit corrections at 4PN, 5PN, and 6PN.
- The nPN expansion of $H_{\text{4PM}}^{\text{hyp}} + \Delta H_{\text{4PM(nPN)}}^{\text{ell}}$ gives the nPN Hamiltonian for bound orbits up to $\mathcal{O}(G^4)$ in isotropic gauge.

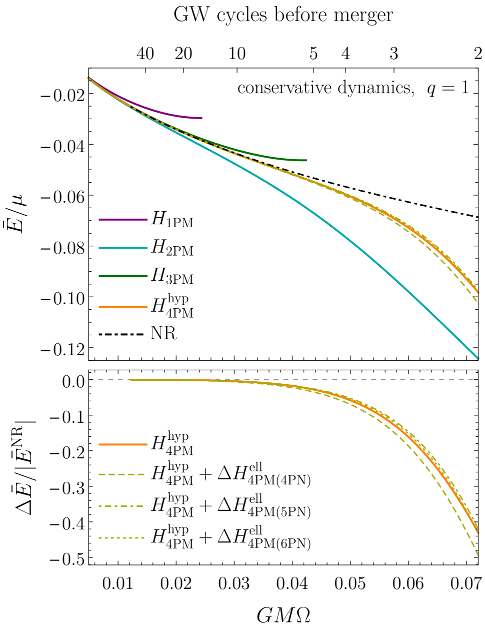

4PM complemented with bound-orbit PN information ($q = 10$)

- Better improvement for $q = 10$, since the 3PN coefficient of the binding energy increases significantly with mass ratio.

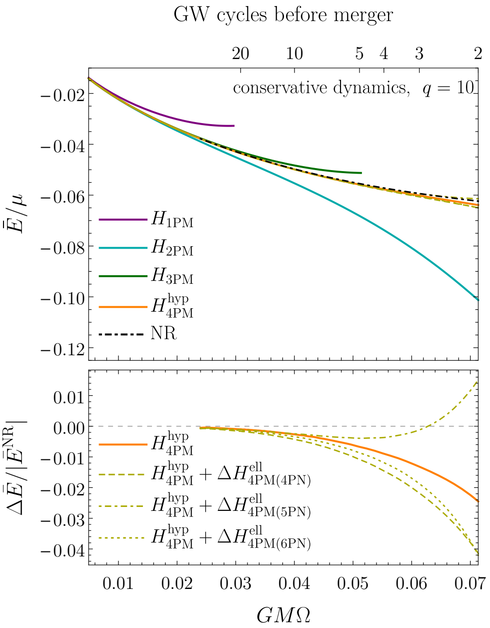

PM-expanded scattering angle

- The scattering angle is gauge invariant, contains the same information as H^{hyp}

$$\chi = -\frac{\partial I_r^{\text{hyp}}}{\partial J}.$$

- NR simulations for equal masses, initial velocity $v \simeq 0.4$, NR error $\sim 1-2$ deg.
  [Damour, Guercilena, Hinder, Hopper, Nagar, Rezzolla 1402.7307]

- Plotted PM-expanded $\chi(E, J)$, using NR initial values.

- 4PM(3PN) is ~ 0.1 degrees lower than 4PM.

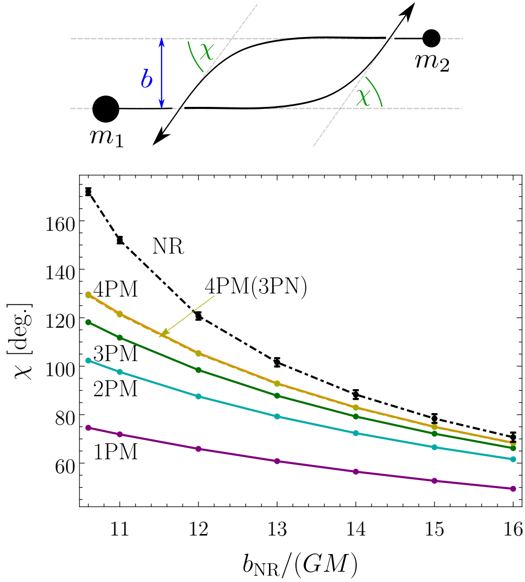

Effect of radiation reaction on the scattering angle

- Radiative contribution to scattering angle, to linear order in radiation reaction (RR)

  [Bini, Damour 1210.2834]

$$\chi^{\text{rad.}} = \frac{1}{2}\Big[\chi^{\text{cons.}}(E_{\text{out}}, J_{\text{out}}) - \chi^{\text{cons.}}(E_{\text{in}}, J_{\text{in}})\Big],$$

- Total scattering angle

$$\chi^{\text{tot}} = \chi^{\text{cons.}}(E_{\text{in}}, J_{\text{in}}) + \chi^{\text{rad.}}(E_{\text{in}}, J_{\text{in}}) \simeq \chi^{\text{cons.}}\left(\frac{E_{\text{in}} + E_{\text{out}}}{2}, \frac{J_{\text{in}} + J_{\text{out}}}{2}\right)$$

- E_{out} and J_{out} obtained from NR.

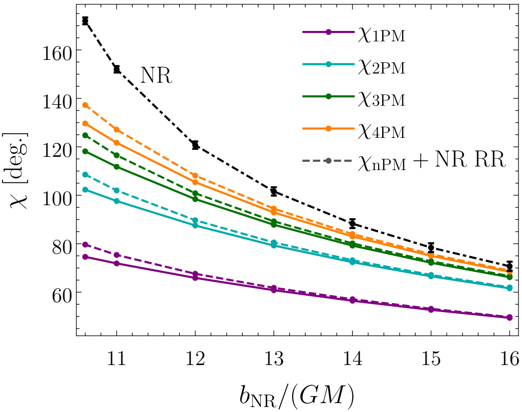

Effective-one-body (EOB) formalism

- EOB maps the binary motion to that of a test mass in a deformed Schwarzschild background [Buonanno, Damour 9811091]

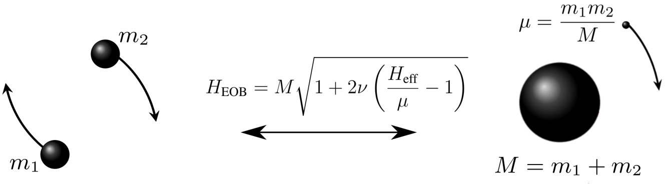

Effective-one-body (EOB) formalism

- EOB maps the binary motion to that of a test mass in a deformed Schwarzschild background [Buonanno, Damour 9811091]

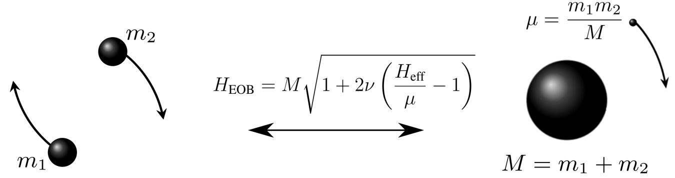

- Effective background metric and mass-shell condition

$$g^{\text{eff}}_{\mu\nu} \mathrm{d}x^\mu \mathrm{d}x^\nu = -A\mathrm{d}t^2 + B\mathrm{d}r^2 + r^2\left(\mathrm{d}\theta^2 + \sin^2\theta \mathrm{d}\phi^2\right)$$

$$0 = g^{\mu\nu}_{\text{eff}} p_\mu p_\nu + \mu^2 + Q$$

- Effective Hamiltonian $H_{\text{eff}} = E_{\text{eff}} = -p_0$

$$H_{\text{eff}} = \sqrt{A\left(\mu^2 + \frac{p_r^2}{B} + \frac{J^2}{r^2} + Q\right)}$$

H_{eff} reduces to the Schwarzschild Hamiltonian as $\nu \to 0$

$$H_S^2 = (1-2u)\left[\mu^2 + (1-2u)\,p_r^2 + \frac{J^2}{r^2}\right], \qquad u \equiv \frac{GM}{r}$$

PM-EOB Hamiltonians

- EOB energy map with H_S as the effective Hamiltonian reproduces the 1PM two-body Hamiltonian. [Damour 1609.00354]

- Ansatz for PM-EOB Hamiltonian in post-Schwarzschild (PS) gauge
[Damour 1710.10599], [Antonelli, Buonanno, Steinhoff, van de Meent, Vines 1901.07102]

$$(\hat{H}^{\text{eff,PS}})^2 = (1-2u)\left[\mu^2 + (1-2u)p_r^2 + \frac{J^2}{r^2} + u^2 q_{\text{2PM}} + u^3 q_{\text{3PM}} + u^4 q_{\text{4PM}}\right]$$

- Ansatz in PS* gauge

$$(\hat{H}^{\text{eff,PS}^*})^2 = \left(1 - 2u + u^2 a_{\text{2PM}} + u^3 a_{\text{3PM}} + u^4 a_{\text{4PM}}\right)\left[\mu^2 + (1-2u)p_r^2 + \frac{J^2}{r^2}\right]$$

- q_{nPM} and a_{nPM} are determined by matching the scattering angle computed from the EOB Hamiltonian to χ_{4PM}

$$\chi = -2\int_{r_0}^{\infty} \frac{\partial p_r(E,J,r)}{\partial J} dr - \pi$$

- Energy in q_{nPM} and a_{nPM} is replaced with EOB Hamiltonian at lower PM orders to obtain $H_{\text{EOB}}(r, p_r, J)$.

Binding energy from PM-EOB Hamiltonians

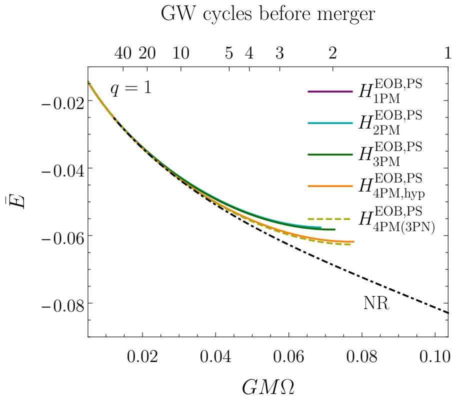

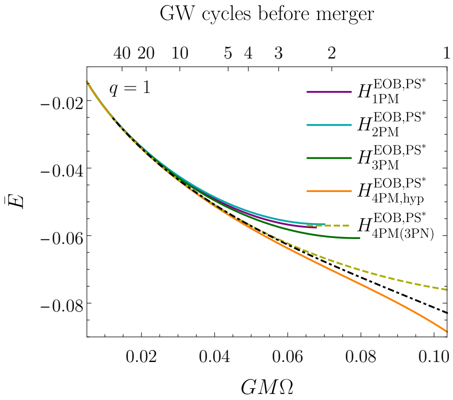

- The PS* gauge is more accurate than the PS gauge
- 3PN-expanded coefficients give slightly better agreement with NR than the full hyperbolic-orbit 4PM

Scattering angle from PM-EOB Hamiltonians

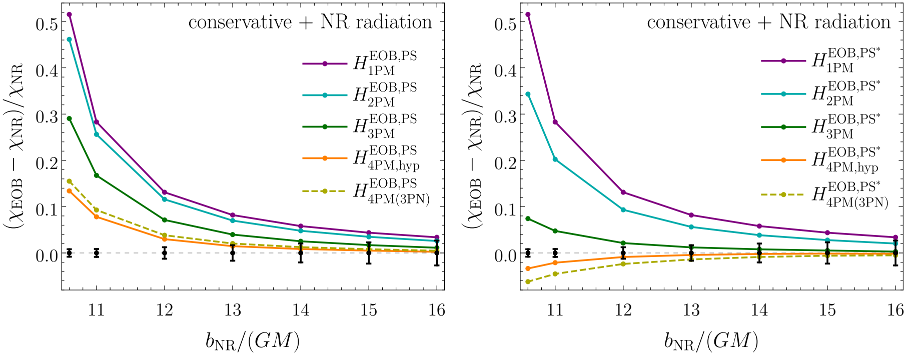

- Scattering angle is calculated by evolving the equations of motion numerically and reading off the final angle ($\chi_{\text{EOB}} = \phi_{\text{out}} - \phi_{\text{in}} - \pi$).
- The full hyperbolic-orbit 4PM Hamiltonian gives better agreement with NR than the 3PN expansion of its coefficients.

Conclusions

- Investigated the conservative 4PM dynamics, showing that the hyperbolic piece has a small effect.
- Compared PM results with NR simulations, finding that PM is comparable to PN for bound orbits, but can perform better for scattering encounters.
- Incorporated PM information in EOB Hamiltonians, leading to significantly better results.
- Possible future work:
  - Produce NR scattering simulations with unequal masses and higher energy
  - Develop waveform model for scattering based on PM results
  - Include spin in a PM-EOB Hamiltonian